The 13th Japan-US Workshop on HIF and HEDP
@ILE, Osaka University

Heavy-Ion Stopping Calculation for Warm Dense Targets Using Dielectric Response Functions

14 October 2011

Yoshiyuki Oguri
Research Laboratory for Nuclear Reactors,
Tokyo Institute of Technology

Temperature/density-dependent heavy-ion stopping data are important for ion-driven WDM experiments.

- Concept of the ion-driven WDM experiment planned by US-HIFS-VNL[1]:

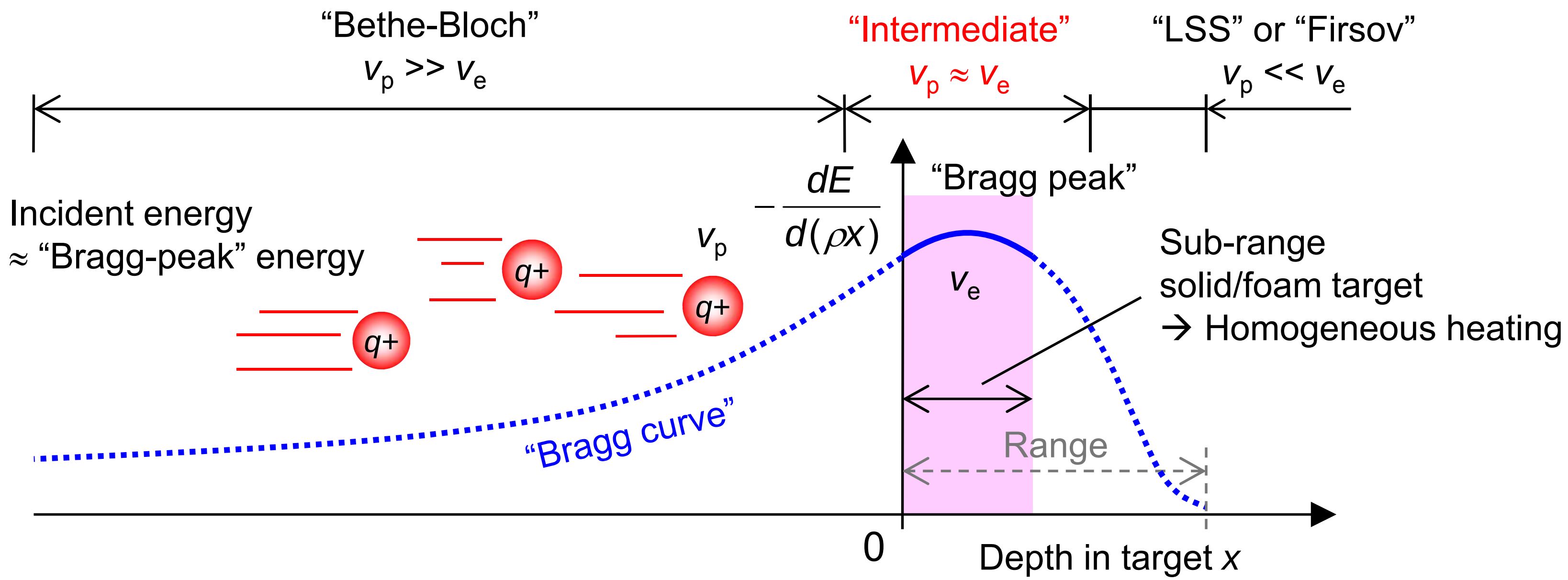

- However, the Bragg curve shape can change during irradiation owing to
  - increase of temperature,
  - decrease of density (if hydro expansion is not negligible).

→ Hydro calculation with temperature/density-dependent stopping data is necessary for detailed design of the experimental conditions.

[1]B. G. Logan, *"Progress of heavy ion fusion science towards warm dense matter physics"*, Workshop on accelerator driven warm dense matter physics, Pleasanton, CA, February 22-24, 2006.

In the previous calculation, collective excitation of the target electrons was not taken into account.

- Previous calculation (US-J WS2008) ← Classical binary collision model:
  - The projectile is assumed to be a point charge *q*+
  - Total interaction = sum of many classical binary close collision

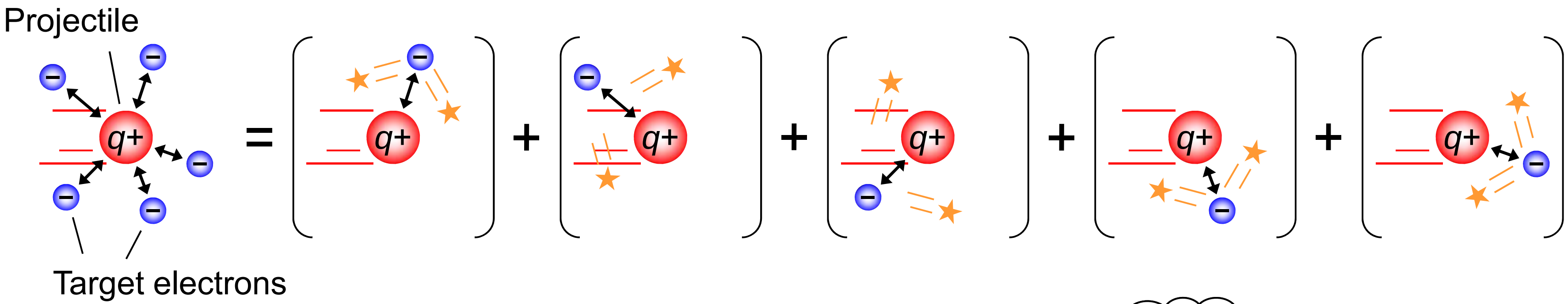

- Limitations:
  - No quantum effects
  - No collective excitation of the target electrons as a plasma
  - No anti-screening of projectile nuclear charge

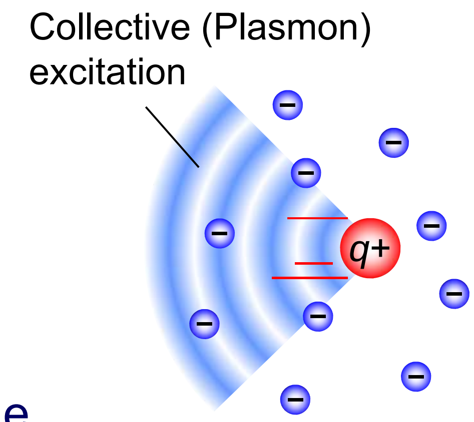

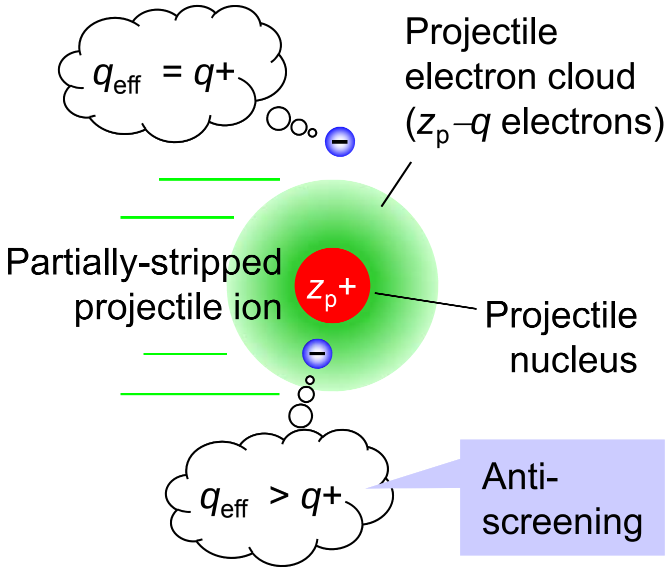

The stopping calculation was performed based on a similar way to the Ziegler's method[2].

- Brandt-Kitagawa[3] effective-charge theory:
  - Electronic stopping cross section:

$$S_e = \frac{z_p^2 e^4}{4\pi\varepsilon_0^2 m v_p^2} \int_0^{R_{WS}} n_e(r) L(r) \cdot 4\pi r^2 dr, \qquad R_{WS} = \sqrt[3]{\frac{3}{4\pi N_{atom}}}$$

Wigner-Seitz radius

  - "Stopping number"

Wave-number representation of $\rho(r)$

$$L(r) = \frac{i}{\pi \omega_p(r)^2} \int_0^{\infty} \frac{dk}{k} \left| \frac{\hat{\rho}(k)}{z_p} \right|^2 \int_{-kv_p}^{kv_p} \omega d\omega \, \mathrm{Im}\left(\frac{-1}{\varepsilon(k,\omega)} \right)$$

$\varepsilon(k, \omega) \equiv$ Dielectric response function of the electron plasma

↓↑

Collective excitation

  - Local plasma frequency:

$$\omega_p(r) = \sqrt{\frac{e^2 n_e(r)}{\varepsilon_0 m}}$$

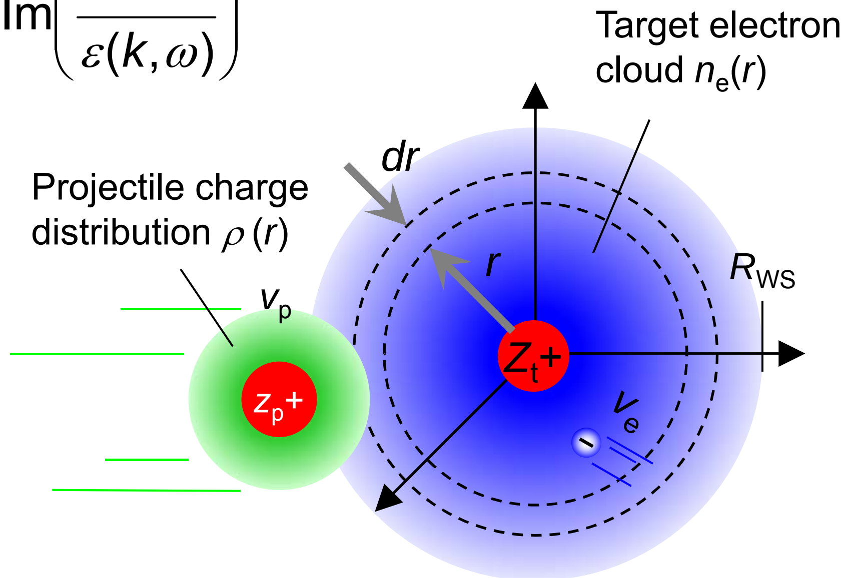

[2] J.F. Ziegler, J.P. Biersack and U. Littmark, *The Stopping and Range of Ions in Solids*, Pergamon Press, ISBN 0-08-021603 (1985).
[3] W. Brandt and M. Kitagawa, *Phys. Rev.* B **25** (1982) 5631.

Quantum mechanical dielectric response functions were used to treat arbitrary plasma degeneracies.

- Temperature/density-dependent dielectric response function by Arista[4]:

$$\varepsilon(k,\omega) \equiv \varepsilon_{\mathrm{Re}}(k,\omega) + i\varepsilon_{\mathrm{Im}}(k,\omega)$$

$$\varepsilon_{\mathrm{Im}}(k,\ \omega)\begin{cases} \neq 0 \rightarrow \text{Close binary collision} \\ = 0 \rightarrow \text{Collective (Plasmon) excitation} \end{cases}$$

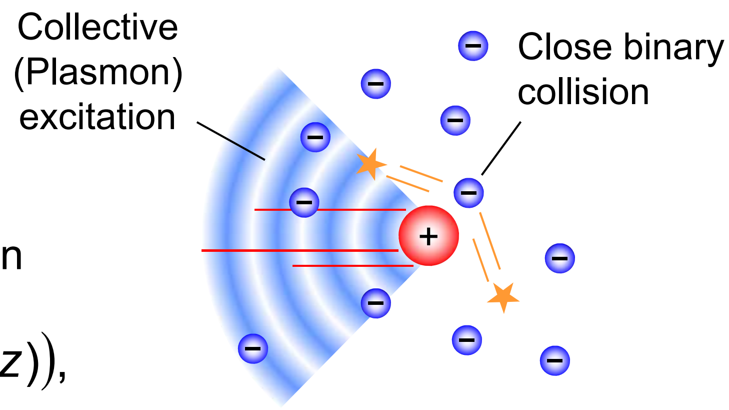

- Real part:

$$\varepsilon_{\mathrm{Re}}(k,\omega) = 1 + \frac{\chi_0^2}{4z^3}\left(g(u+z) - g(u-z)\right),$$

$$z \equiv \frac{k}{2k_{\mathrm{Fermi}}},\quad u \equiv \frac{\omega}{k v_{\mathrm{Fermi}}},\quad \chi_0^2 \equiv \frac{v_{\mathrm{Bohr}}}{\pi v_{\mathrm{Fermi}}},$$

$$g(x) \equiv \int_0^\infty \frac{y\,dy}{e^{Dy^2-\eta}+1}\ln\left|\frac{x+y}{x-y}\right| = -g(-x)$$

- Imaginary part:

$$\varepsilon_{\mathrm{Im}}(k,\omega) = \frac{\pi\chi_0^2}{8z^3}\left(\frac{1}{D}\right)\ln\left\{\frac{1+e^{\eta-D(u-z)^2}}{1+e^{\eta-D(u+z)^2}}\right\}$$

Plasma degeneracy

$$\eta \equiv \frac{\mu}{k_{\mathrm{B}}T},\quad D \equiv \frac{E_{\mathrm{Fermi}}}{k_{\mathrm{B}}T}$$

Temperature/density dependence

[4]N. R. Arista and W. Brandt, *Phys. Rev.* A **29** (1984) 1471.

The Brandt-Kitagawa theory[3] was adopted to calculate the projectile effective charge.

- Screening/anti-screening effect was taken into account by assuming the projectile charge density distribution $\rho(r)$:

$$\rho(r) = z_p \delta(r) - \frac{N_{\text{bound}}}{4\pi\Lambda^3}\left(\frac{\Lambda}{r}\right)e^{-r/\Lambda} \xrightarrow{\text{Fourier transform}} \hat{\rho}(k) = z_p\left\{\frac{q+(k\Lambda)^2}{1+(k\Lambda)^2}\right\}$$

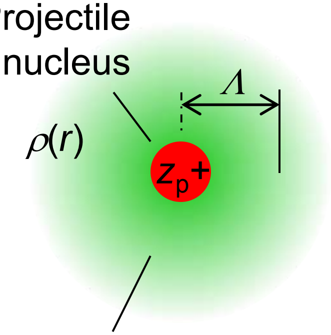

  - Screening length:

$$\Lambda = \frac{0.48\left(N_{\text{bound}}/z_p\right)^{2/3}}{z_p^{1/3}\left\{1-\left(N_{\text{bound}}/z_p\right)/7\right\}}$$

- Projectile charge state:

$$q = z_p\left\{1 - e^{-0.95(y_{\text{rel}}-0.07)}\right\}, \qquad y_{\text{rel}} \equiv \frac{v_{\text{rel}}}{v_{\text{Bohr}} z_p^{2/3}}$$

Relative velocity between the projectile and target electrons

$$v_{\text{rel}} = \frac{\left(v_p + v_{ve}\right)^3 - \left|v_p - v_{ve}\right|^3}{6 v_p v_{ve}}$$

Averaged target-electron velocity

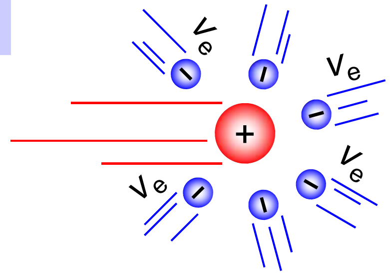

  - BK's recipe: v_{ve} must be the averaged velocity only of "valence" electrons (not of all the electrons) → The "core" must be excluded!

[3]W. Brandt and M. Kitagawa, *Phys. Rev.* B **25** (1982) 5631.

A Thomas-Fermi model was used to evaluate the target electron density/velocity distribution.

- Temperature-dependent Thomas-Fermi model:
  - $e\phi(r)$ = electrostatic potential
  - μ = chemical potential

$$f_e(r,v_e) \equiv \left(\frac{1}{m\pi^2\hbar^3}\right)\frac{1}{1+\exp\left(\frac{mv_e^2/2 - e\phi(r) - \mu}{k_B T}\right)}$$

Phase-space distribution

→ No shell structure, no distinction between the core- and valence electrons

- The TF target atom was separated into the core and valence parts using Cappeluti's method[5]:
  - Total energy stored in a sphere with a radius r:

$$W(r) \equiv \int_0^r \left(w_{kin}(r') + w_{ei}(r') + w_{ee}(r')\right) 4\pi r'^2 \, dr',$$

$$w_{kin}(r) \equiv \int_0^\infty \frac{m_e v_e^2 (r)^2}{2} dv_e, \quad w_{ei}(r) \equiv -\frac{Ze^2}{4\pi\varepsilon_0} n_e(r),$$

$$w_{ee}(r) \equiv \frac{1}{2}\left(\frac{e^2}{4\pi\varepsilon_0}\right) n_e(r) \int_{r'}^{R_{WS}} \frac{n_e(r')}{|r - r'|} dr'.$$

  - The core-valence boundary is given by r_c where $W(r)$ has the minimum.

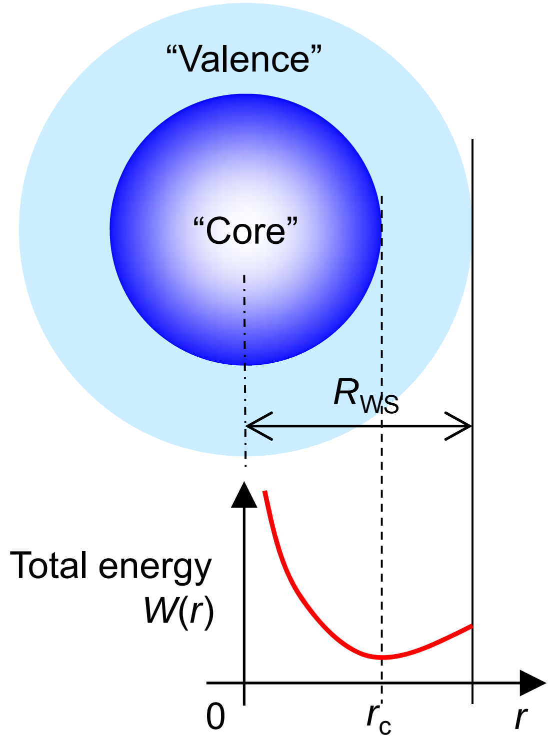

[5]E. Cappelluti and L. Delle Site, *Physica* A **303** (2001) 481.

The target electron density distribution changes with the temperature and pressure.

- Temperature/density-dependence of $n_e(r)$ in an $_{13}$Al target atom:

Density	Temp. kT (eV)	Press. P (Mbar)	Ioniz. deg. η	Plasma coup. const. Γ
$3\rho_{solid}$	0.025	12	42%	925
	25	38	44%	0.94
$10^{-4}\rho_{solid}$	0.025	2.8×10^{-8}	1.1%	8.72
	25	1.8×10^{-3}	58%	0.033

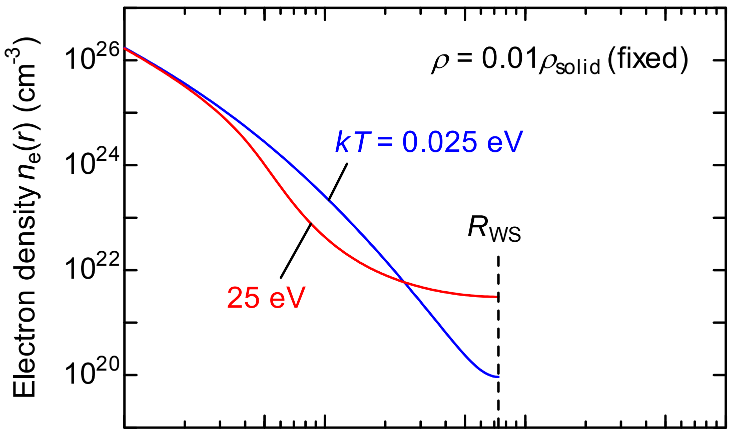

- Comparison with a HF calculation:

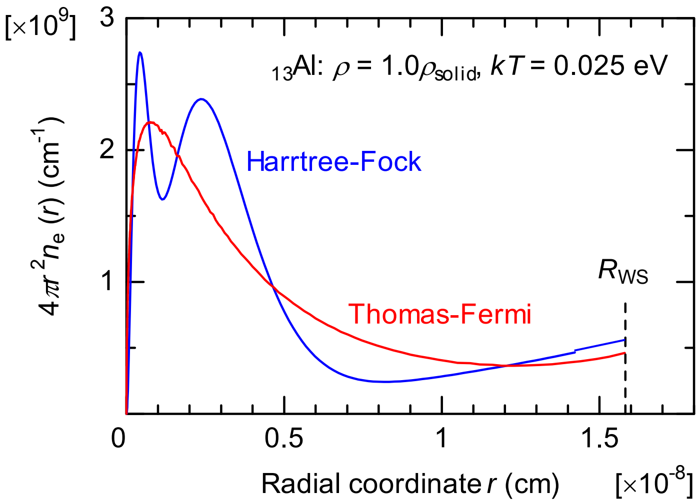

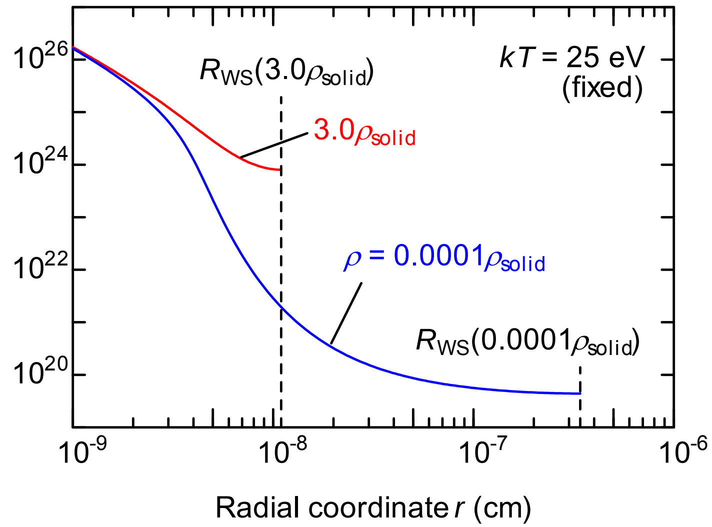

The accuracy for the cold solid target became a bit worse than before, although the model was improved.

- Result of calculation; comparison with other data :
  - $_{11}$Na projectile, $_{13}$Al target
  - Total stopping S = Electronic stopping S_e + Nuclear stopping[6] S_n ($S_n << S_e$)
  - Asymptotic behaviors ($E < \approx$ 30 keV/u, $\approx$ 5 MeV/u $< E$) are excellent.

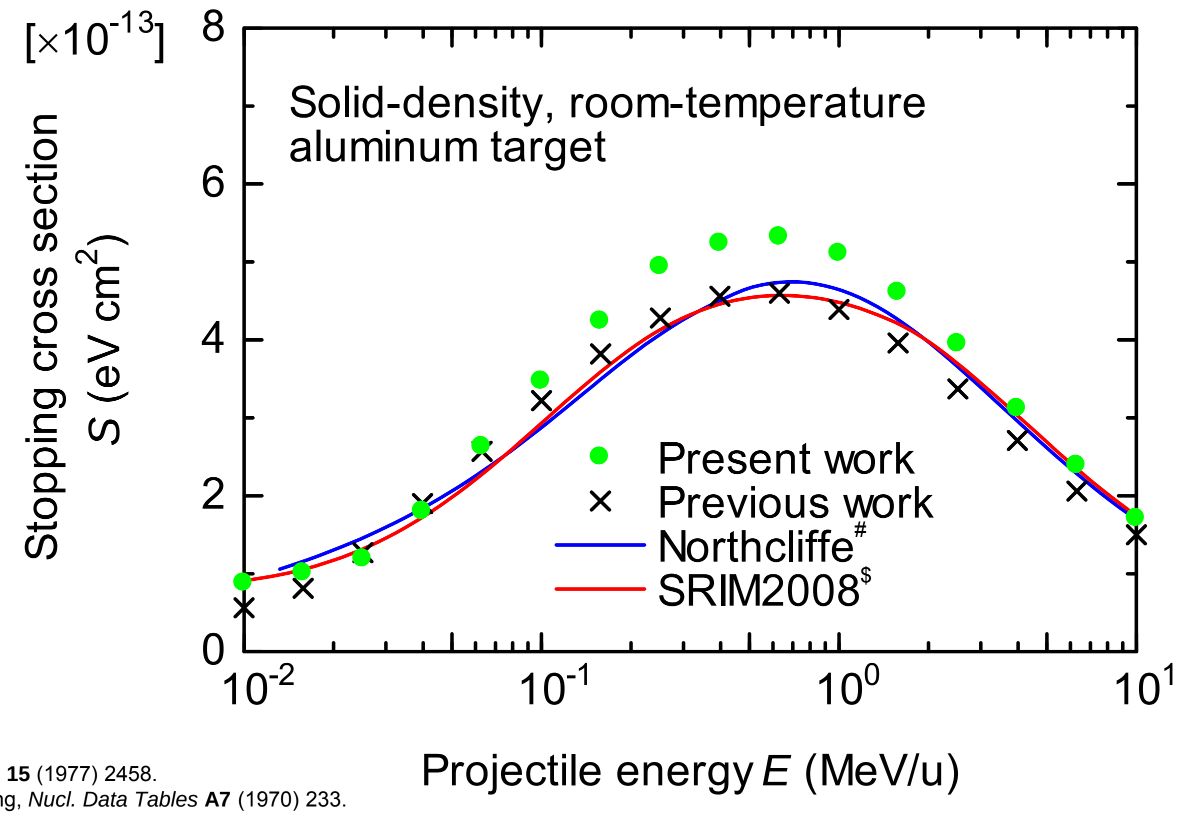

[6]W. D. Wilson et al., *Phys. Rev.* B **15** (1977) 2458.
[#]L. C. Northcliffe and R. F. Schilling, *Nucl. Data Tables* **A7** (1970) 233.
[$]J. F. Ziegler, *"Computer Code SRIM-2008"*, URL: http://www.srim.org/.

The projectile stopping power increases with increasing temperature and decreasing density of the target.

- Temperature/density-dependence of the stopping cross-section for $_{13}$Al:

Temperature dependence

Density dependence

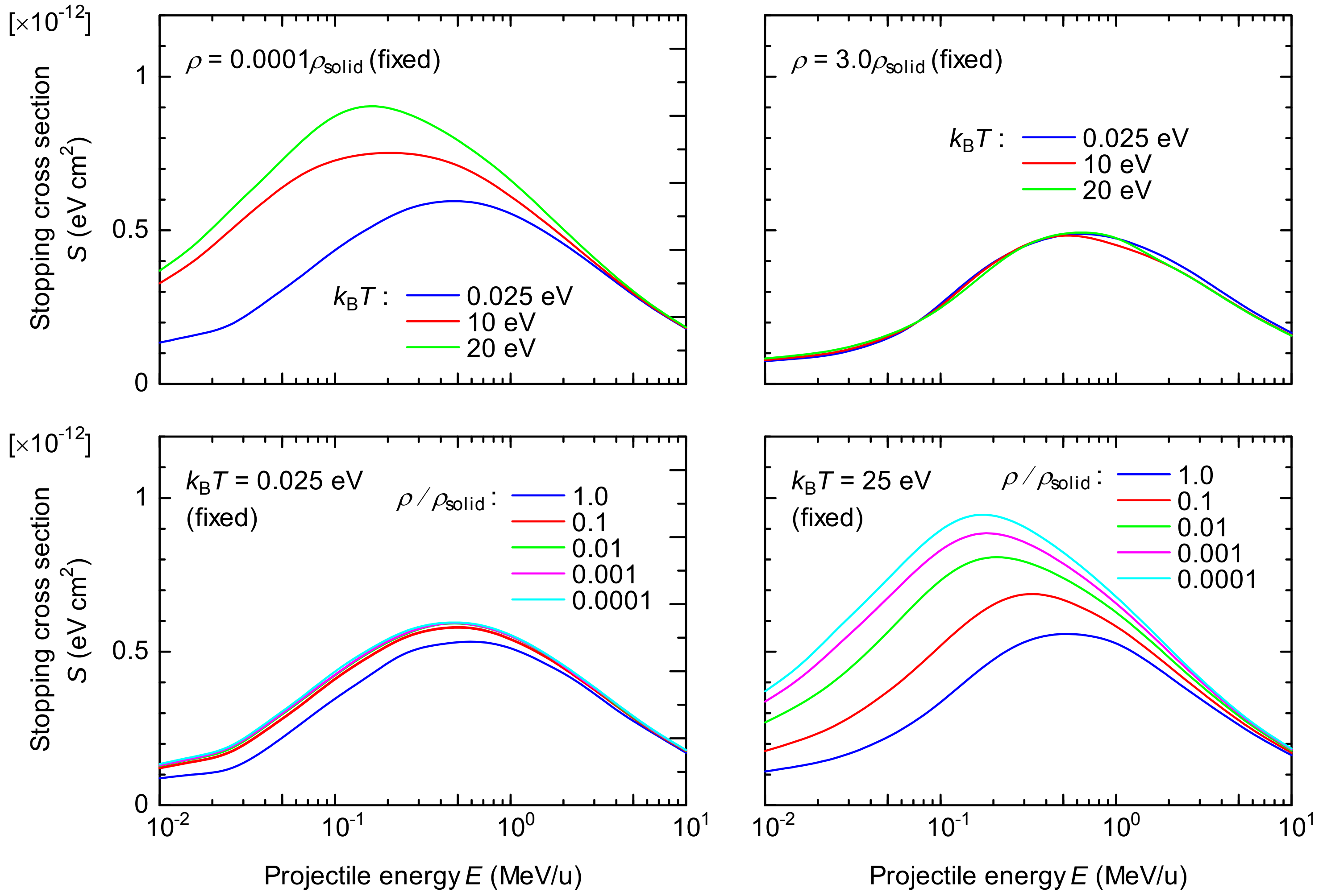

The target thickness and projectile energy were designed based on the data for cold solid Al target.

- An example for demonstration of the temperature/density effect:
  - Projectile: 30.6-MeV $^{23}Na^{+}$ (1.33 MeV/u), 30 GW/mm^2 (peak) × 1 ns (FWHM)
    → Energy per pulse W = 30 J/mm^2 (1.7×10^{13} ions/mm^2)
    (Not achievable even by the future VNL IB-HEDPX):
  - Target: $_{13}$Al-slab, thickness = 2.3 mg/cm^2
  - $-dE/d(\rho x)$-inhomogeneity = ± 5%, if the cold solid Al data are used.

Target	(Solid)	Foam	Foam
Density (ρ / ρ_{solid})	(1.00)	0.1	0.01
Thickness (μm)	(8.36)	83.6	836

$$P(t) = P_{peak} \sin^2\left(\frac{\pi t}{2\tau}\right)$$

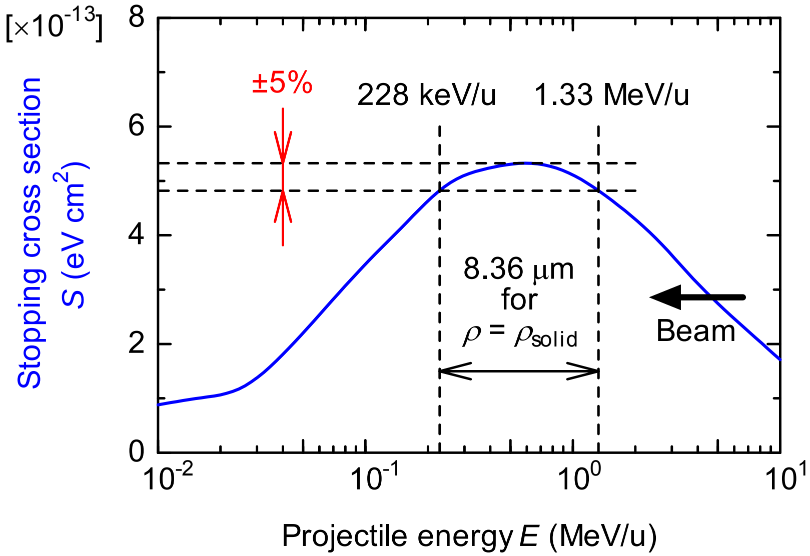

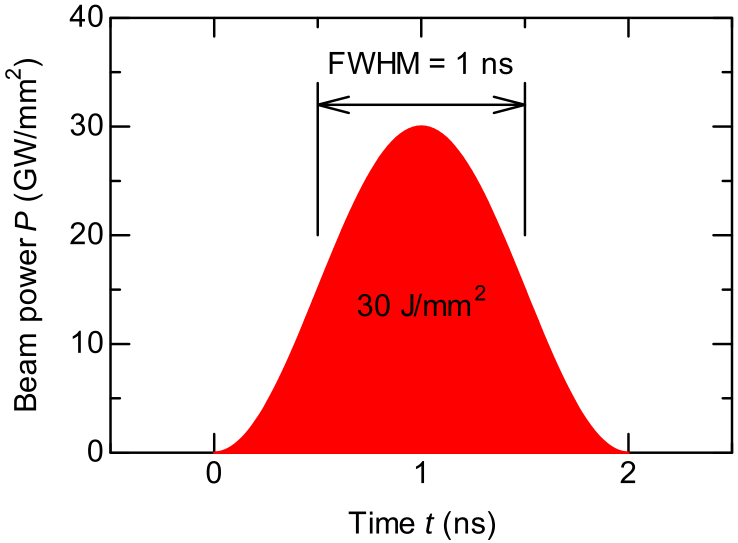

Hydro motion of the target was analyzed using a 1D code being coupled with the stopping data.

- Original hydro code summary:
  - "MULTI (MULTIgroup radiation transport in MULTIlayer foils)"[7], version 7 by Rafael Ramis (MPQ, Garching)
  - 1D radiation hydrodynamics
  - Fully implicit Lagrangian scheme
  - Time-splitting algorithm
  - Tabulated EOS data (SESAME table)
- Modifications made by this work:
  - Laser deposition routine was canceled.
  - Original ion beam deposition routine (constant *dE/dx*!) was modified to use a *dE/dx* (E,ρ,kT) table prepared by the present methods.
  - Heat conductivity: Classical heat flux by Spitzer → SESAME table

[7] R. Ramis, R. Schmalz and J. Mayer-ter-Vehn, *Computer Physics Communications* **49** (1988) 475.

The target hydro motion can be affected by the temperature/density dependence of the stopping.

- Temporal evolution of *kT* and $-dE/\rho dx$ during irradiation ($t < 2$ ns):

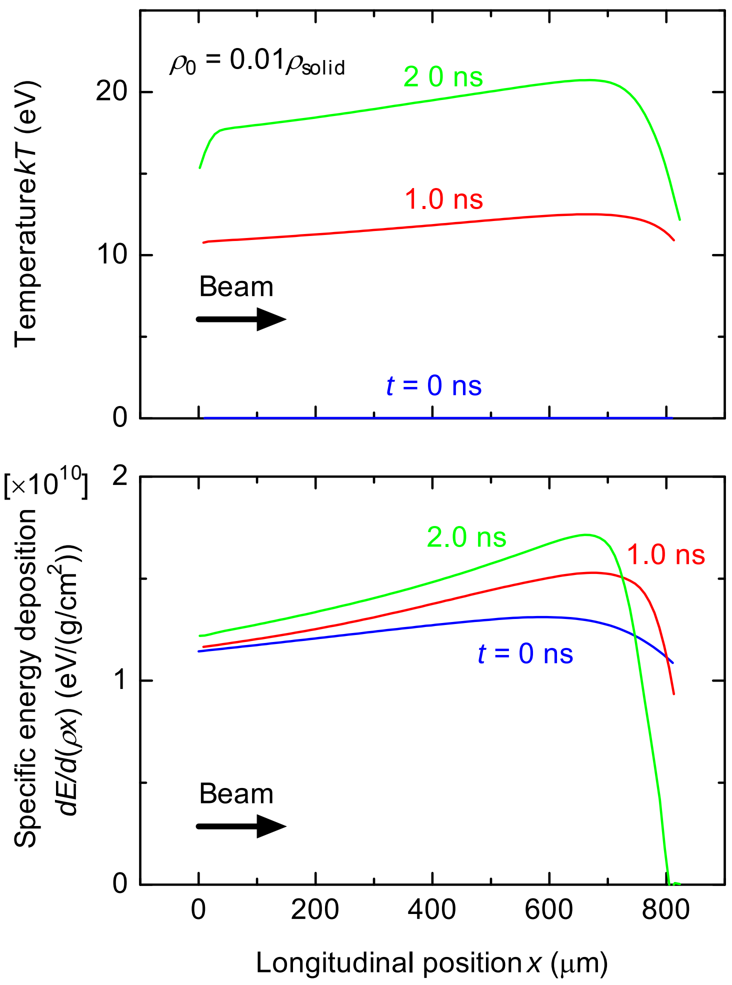

- Hydro motion after irradiation ($t > 2$ ns):

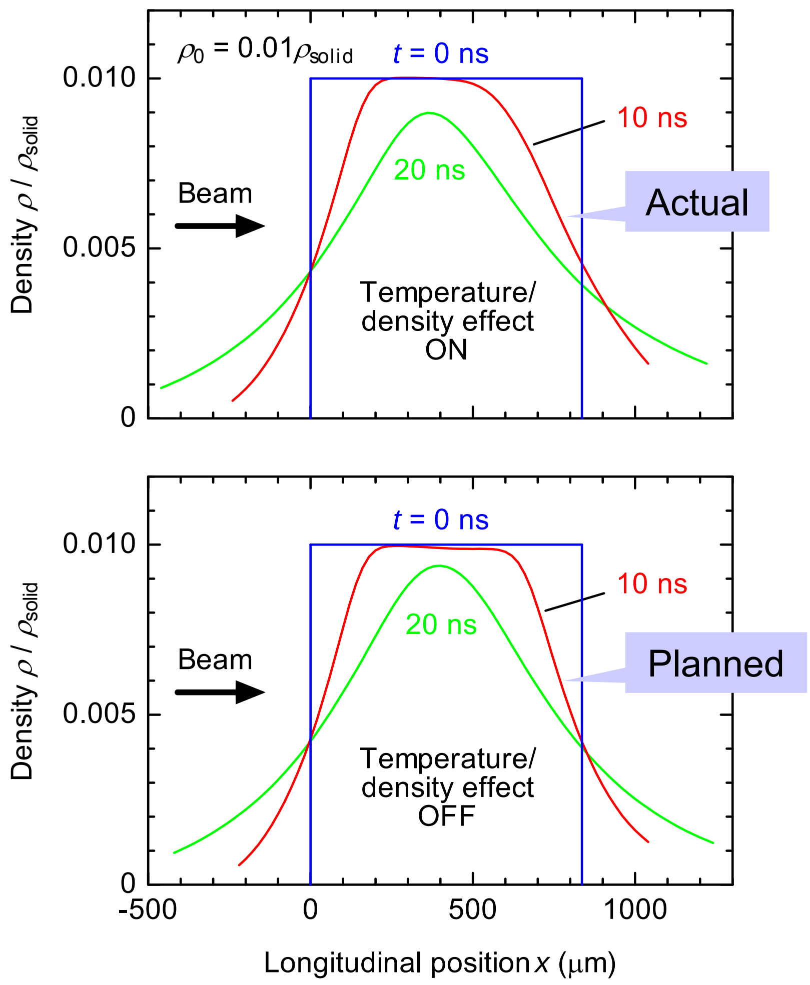

If the peak power is reduced to < 10 GW/mm^2, the heating homogeneity can be improved.

- Beam power dependence (t = 2 ns):

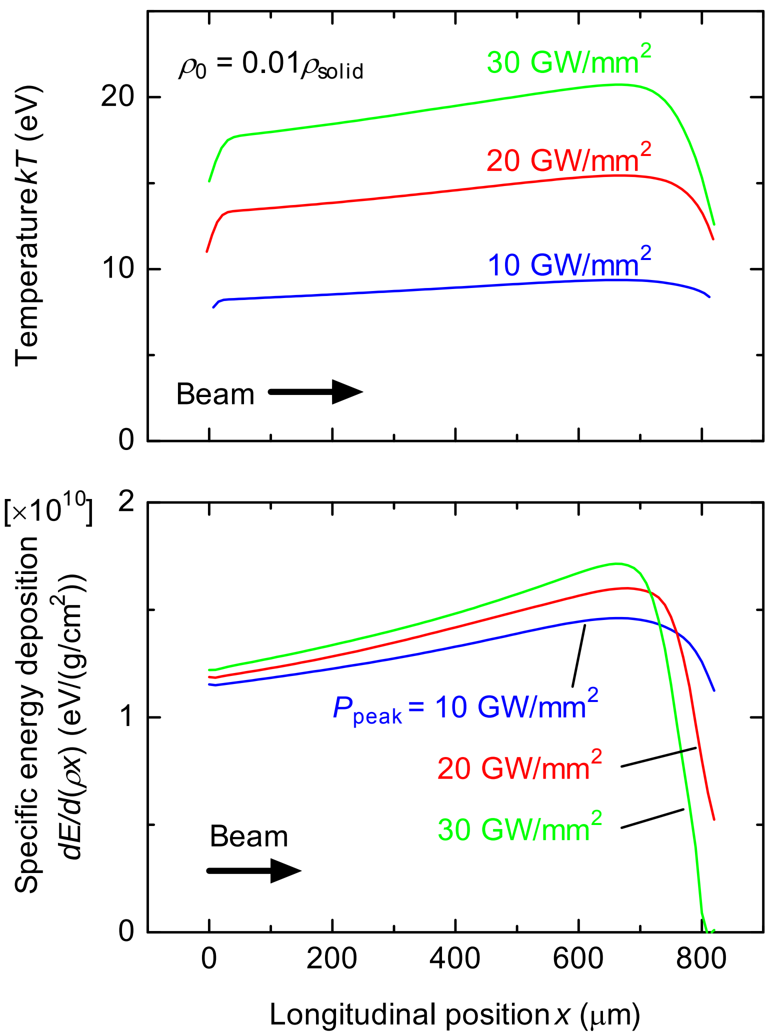

- cf. Previous results:

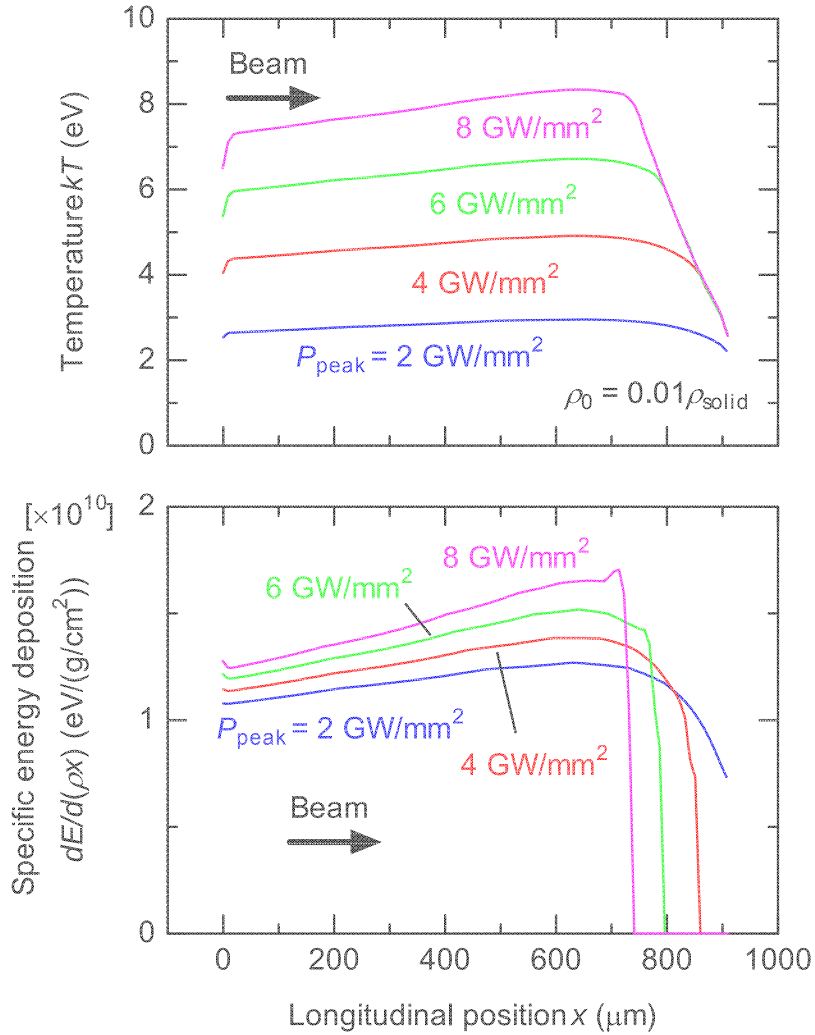

Conclusions: The projectile stopping calculation was improved and successfully embedded in the hydro code.

- Projectile stopping calculation using the quantum dielectric response theory:
  - Temperature/density dependence of the stopping showed a similar tendency to the previous calculations based on the classical binary collision model.
  - The temperature/density effects became less significant than those by the previous calculations.
- Hydro calculation regarding the Bragg-peak-based US-WDM experiment:
  - Consideration on the temperature/density effect might not be necessary, if the $_{11}$Na-beam power is less than ≈ 10 GW/mm^2 (or kT < 10 eV).